Spatiotemporal variations of multi-scale drought in Shandong Province from 1961 to 2017

Tian Yao, Qiang Zhao, Xin-ying Li, Zhen-tao Shen, Peng-yu Ran and Wei Wu

ABSTRACT

Drought has caused serious damage to the water resource system and agricultural production in Shandong Province, China. This study calculated the standardized precipitation evapotranspiration index (SPEI) based on the monthly precipitation and average temperature data of 25 meteorological stations in Shandong Province from 1961 to 2017. The trend analysis method and ArcGIS software were utilized to analyze the multi-scale (SPEI-1, SPEI-3, and SPEI-12) spatiotemporal changes of drought. The results revealed that (1) The intensity of drought showed an increasing trend in Shandong Province from 1961 to 2017; (2) The main periods of the drought on the seasonal scale (spring, summer, autumn, and winter) and annual scale were 8 years, 4 years, 15 years, 4 years, and 4 years, respectively; (3) Of the four seasons, the frequency of drought in autumn and winter were the highest. At the annual scale, the high-frequency drought areas were mainly concentrated in the southern mountainous regions; (4) In terms of the spatial change trend of drought, Shandong Province as a whole displayed a trend of becoming wet in the central and southwest regions and dry in the eastern region; and (5) Droughts were discovered to be simultaneously influenced by multiple atmospheric circulation indices in Shandong Province.

Key words | drought, Shandong Province, spatial-temporal evolution, SPEI

Tian Yao
Qiang Zhao (corresponding author)
Xin-ying Li
Zhen-tao Shen
Peng-yu Ran
Wei Wu
School of Water Conservancy and Environment,
University of Jinan,
Jinan 250022,
China
E-mail: *zhaoqiang8827@sina.com*

HIGHLIGHTS

- The intensity of drought showed an increasing trend.
- The spatial distribution of drought in Shandong Province varies greatly at different scales.
- The aridity trend across the entire province in autumn.
- Droughts in Shandong Province were simultaneously affected by multiple atmospheric circulation indices.

doi: 10.2166/ws.2020.332

GRAPHICAL ABSTRACT

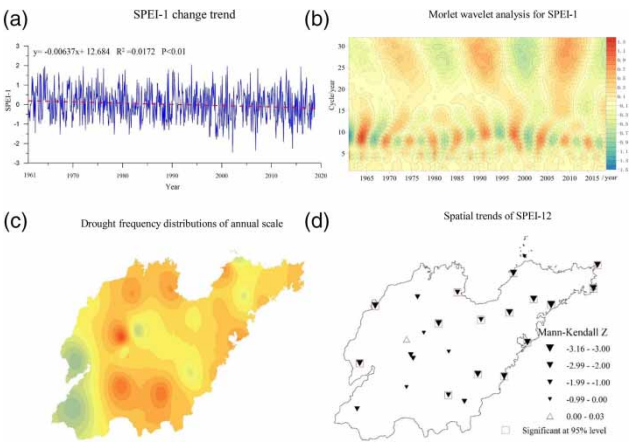

INTRODUCTION

Global climate change has become one of the most complex challenges facing mankind in the 21st century and is seriously impacting both the regional ecological environment and the sustainable development of human society (Schär *et al.* 2016). Of these effects, the warming of the climate has increased the surface evapotranspiration and precipitation in a strongly regional way (Bongaarts 2018), resulting in significant increases in the frequency and intensity of extreme climate events such as high temperatures, floods, and droughts (You *et al.* 2011; Li *et al.*, 2020). Among the many types of extreme climate crises, drought, as the most common natural disaster, displays the characteristics of high frequency, long duration, wide range of impact, and so on (Aghakouchak *et al.* 2014). Droughts affect more people than any other hazard, they are one of the main natural hazards regarding their economic and environmental impacts, with negative effects on industrial production, citizens' lives, ecological environment, extension of forests or vegetation activity (Hayes *et al.* 2011; Cook *et al.* 2014; Hao *et al.* 2014). Droughts also lead to a shortage of water resource, impact agricultural production, affect the safety of domestic water for residents, and even cause great harm to the ecological environment (Chen *et al.* 2013). As a large agricultural country, China's agriculture is the foundation of its national economy, and drought is the main restricting factor affecting its agricultural economy (Zhang & Diao 2020). Therefore, timely and accurate research on the spatial and temporal distribution characteristics of regional drought will help us to clearly understand the mechanisms of drought evolution and implement drought prevention and mitigation measures both scientifically and effectively.

Many drought indices have been utilized for drought monitoring and research in different regions of the world. The widely used indices include the Palmer drought severity index (PDSI) (Palmer 1965), the standardized precipitation index (SPI) (McKee *et al.* 1993), and the standardized precipitation evapotranspiration index (SPEI) (Vicente-Serrano *et al.* 2010). Wambua *et al.* (2017) used the PDSI to analyze the temporal and spatial variation characteristics of drought in the upper Tana River region of Kenya, which was found to accurately reflect the drought characteristics of the study area. The PDSI, comprehensively considers the influence of antecedent precipitation, soil moisture content, and potential evapotranspiration. However, due to the impact of supply and demand balance, there are disadvantages such as a single time scale and no spatial comparability in practical applications (Guo *et al.* 2018). Vicente-Serrano & López-Moreno (2006) analyzed the temporal and spatial characteristics of winter drought in the semi-arid region of northeast Spain from 1952 to 1999 based on the SPI, accurately reflecting the droughts in that area over the study period. The SPI features the advantages

of simple calculation, multi-time scale characteristics, and spatial comparability, although it ignores the influences of air temperature and evapotranspiration on drought occurrence and has limitations in the exploration of drought problems under climate warming (Guo *et al.* 2018). On the basis of the SPI, Vicente-Serrano proposed a standardized precipitation evapotranspiration index (SPEI) based on precipitation and potential evapotranspiration, which takes into account the statistical distribution of precipitation. The potential evapotranspiration over the same period is also taken into account in order to reflect regional droughts more comprehensively. Yu *et al.* (2014) applied the SPEI to investigate the drought trend in China from 1951 to 2010, concluding that the SPEI has good applicability in drought monitoring and analysis in China; and Tan *et al.* (2015) studied the drought characteristics of the Ningxia Autonomous Region in China with the SPEI, finding that the SPEI is more suitable for climate change and drought change in Ningxia than the SPI.

Shandong Province is located on the east coast of China, in a temperate zone that experiences a strong continental climate. The seasonal differences in precipitation and temperature during the year are very large, exhibiting significant regionalism, diversity, and instability (Jiang *et al.* 2020). At the same time, due to climate warming and the impact of human activities, the risk of natural disasters in Shandong Province has increased, which is seriously impacting the ecological environment and agricultural production (Shi *et al.* 2020). Research on the spatial and temporal distribution of drought in Shandong Province has been performed, although it has mainly focused on the analysis of the spatial and temporal characteristics of drought in small local areas of the province. There have been relatively few studies on the spatial difference of long time series and multi-time scale droughts, or changes in the drought cycle and their influencing factors in Shandong Province. Research on the impact of multiple atmospheric indices on drought in Shandong Province remains relatively insufficient. Therefore, based on the data from 25 meteorological stations in Shandong Province for the period 1961–2017, this study attempted to analyze the spatiotemporal changes of drought and the drought cycle in Shandong Province by calculating the SPEI at different time scales and to discuss the major global and regional atmospheric circulation indices relative to Shandong Province, with the expectation of providing decision-making suggestions for the development of drought early warning systems, as well as agricultural and animal husbandry advancement in Shandong Province.

DATA AND METHODS

Study area

Shandong Province is located on the east coast of China in the lower reaches of the Yellow River, from 34°22.9′ to 38°24.01′N latitude and 114°47.5′E to 122°42.3′E longitude. It consists of peninsulas and inland areas and has a total land area of 156,700 km^2 (Figure 1(a)). The western and northern regions are surrounded by the North China Plain, while the central and eastern areas consist of mountains and hills, with a maximum elevation of 1,517 m. Parts of Shandong Province experience a temperate monsoon climate, while other sections experience a temperate climate. The average annual rainfall was 676.5 mm in Shandong Province, and the annual precipitation exhibited a decreasing trend from 1961 to 2017, at a rate of −10.96 mm/decade ($p = 0.38$) (Figure 2(a)), and the precipitation in most areas of Shandong Province showed a downward trend (23.8% stations passed the 95% confidence significance test) (Figure 3(a)).The average annual temperature is 12–14 °C, the annual temperature change in Shandong Province displayed an overall upward trend, at a rate of 0.33 °C/10a ($p < 0.01$) (Figure 2(b)), there was a significant warming trend across all of Shandong Province (all stations passed the 99% confidence significance test), in which the warming rates of the eastern and southeastern coasts were faster than those of other regions (Figure 3(b)).

Data source and quality control

The meteorological data in this study came from the 'Monthly Dataset of Chinese Surface Climate Data (3.0)' (https://data.cma.cn/) compiled by the Meteorological Information Center of the China Meteorological Administration. This dataset includes 15 meteorological elements from 31 meteorological stations in Shandong Province,

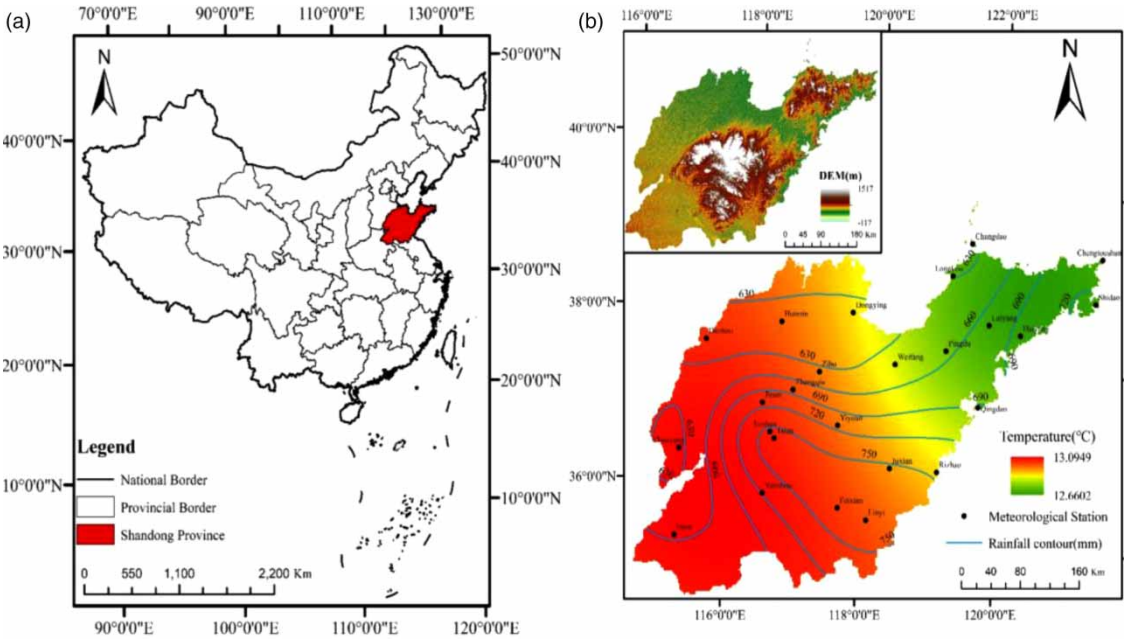

Figure 1 | Geographical location of the study area (a) and weather stations are under (b), as well as the spatial distributions of annual mean temperature, precipitation, and elevation (b).

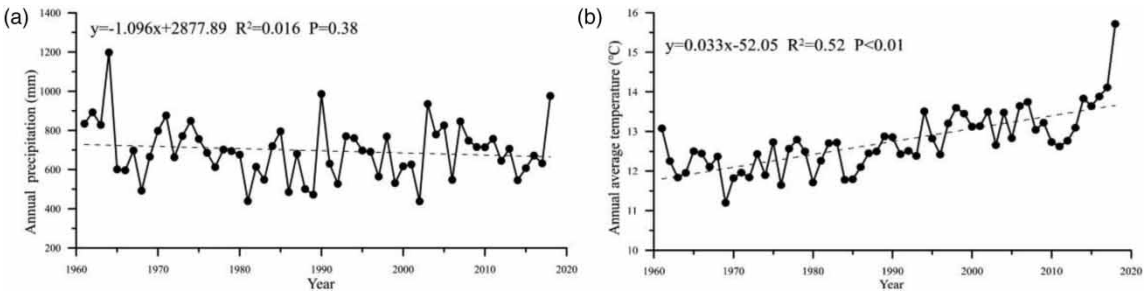

Figure 2 | Changes of rainfall (a) and annual average temperature (b) in Shandong Province from 1961 to 2017.

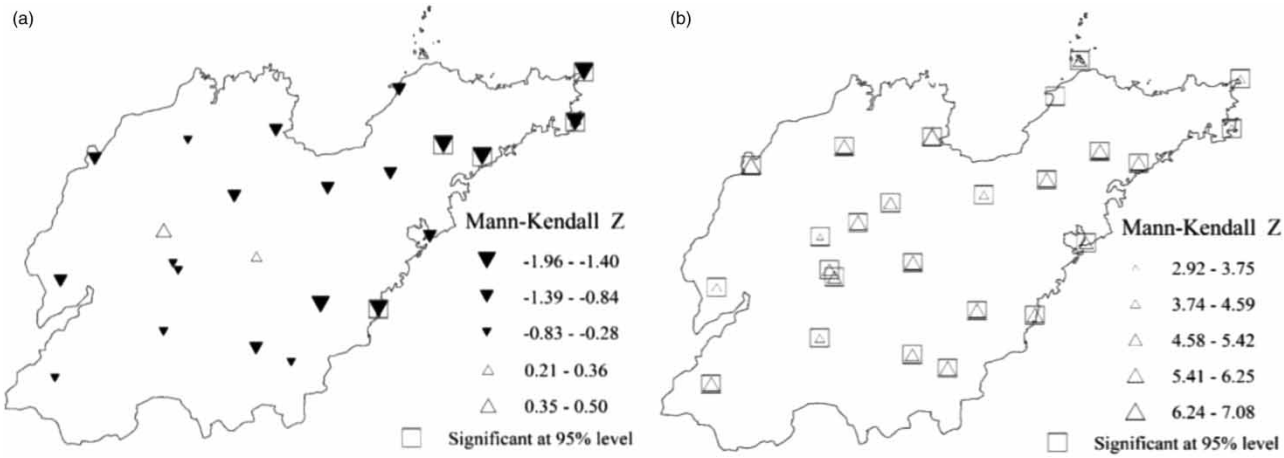

Figure 3 | Spatial trends of rainfall (a) and annual average temperature (b) at 25 stations in Shandong Province from 1961 to 2017.

such as monthly average temperature and monthly rainfall. In this dataset, missing test data are represented as 999999, snowfall is represented as 9996xx, and rain and snow (sleet) are represented as 9997xx. These meteorological data were obtained in strict accordance with the standards of the World Meteorological Organization (WMO) and the technical regulations of the China Meteorological Administration. This dataset has undergone strict quality control and is widely used in climate change-related research in China (Zhao *et al.* 2020). Due to the various observation times of different stations, the relocation of meteorological stations, and other reasons, sections of the dataset may be missing. Therefore, before using this dataset, researchers should conduct quality control again in order to eliminate erroneous or suspicious data. This study conducted data quality control and site selection according to the following principles. (1) The data at a given station should not be <57 years. (2) If a station has >5% temperature and precipitation data missing or data missing for >3 consecutive months, the data will not be utilized. When a small amount of data is lacking from a single station, the interpolation of precipitation and temperature from two or more nearby stations is used to fill the gap, so as to obtain the complete data sequence. (3) Rainfall, snowfall, and sleet are the default precipitation types. Ultimately, the monthly precipitation and average temperature data from 25 meteorological stations were selected from 1961 to 2017 for analysis. According to the international seasonal division principle, March–May was defined as spring, June–August as summer, September–November as autumn, and December–February of the next year as winter.

The basic spatial data of Shandong Province used in this study came from the 30 m × 30 m digital elevation model data downloaded from the Geospatial Data Cloud website (http://www.gscloud.cn/).

Large-scale atmospheric circulation

The large-scale ocean atmospheric circulation indices selected for use in this study included the Arctic Oscillation (AO) (http://www.cpc.ncep.noaa.gov/), Southern Oscillation (SOI) (https://psl.noaa.gov/gcos_wgsp/Timeseries/SOI/), East Asian Summer Monsoon (EASM) (http://ljp.gcess.cn/dct/page/1), North Atlantic Oscillation (NAO) (http://ljp.gcess.cn/dct/page/1), Pacific Decadal Oscillation (PDO) (http://www.esrl.noaa.gov/psd/data/correlation/pdo.data), sunspot number (SN) (http://www.sidc.be/silso/datafiles), and multivariate ENSO index (MEI) (https://www.esrl.noaa.gov/psd/enso/mei/index.html).

Research methods

Standardized precipitation evaporation index

In this study, the SPEI was used to examine droughts in Shandong Province. This index was proposed by Vicente-Serrano *et al.* (2010). The SPEI is mainly constructed from the difference between precipitation and evapotranspiration. The calculation process is as follows.

First, potential evapotranspiration (PET) is calculated (Vicente-Serrano *et al.* 2010):

$$PET_i = 16 * \left(\frac{10T_i}{H}\right)^A (T_i > 0), \tag{1}$$

where A represents a constant, H refers to the annual heat index, and T_i represents the 30-day average temperature. The constants H and A are calculated as follows:

$$H = \sum_{i=1}^{12} H_i = \sum_{i=1}^{12} \left(\frac{T_i}{5}\right)^{1.514} \tag{2}$$

$$A = 6.75 * 10^{-7} H^3 - 7.71 * 10^{-5} H^2 + 1.792 * 10^{-2} H + 0.49. \tag{3}$$

Second, the differences between monthly precipitation and evapotranspiration are calculated as

$$D_i = P_i - PET_i, \tag{4}$$

where D_i represents the difference between precipitation and evapotranspiration, and P_i and PET_i refer to monthly precipitation and evapotranspiration, respectively.

Third, the D_i data are sequentially normalized. D_i is fitted using a log-logistic probability distribution F(x), which is defined as follows:

$$\mathrm{F}(x) = \left[1 + \left(\frac{\alpha}{x - \gamma}\right)^{\beta}\right]^{-1} \tag{5}$$

where α, β, and γ are obtained by linear fitting, via the following calculations:

$$\alpha = \frac{(\omega_0 - 2\omega_1)\beta}{\Gamma\left(1+\frac{1}{\beta}\right)\Gamma\left(1-\frac{1}{\beta}\right)} \tag{6}$$

$$\beta = \frac{2\omega_1 - \omega_0}{6\omega_1 - \omega_0 - 6\omega_2} \tag{7}$$

$$\gamma = \omega_0 - \alpha\Gamma\left(1+\frac{1}{\beta}\right)\Gamma\left(1-\frac{1}{\beta}\right), \tag{8}$$

where Γ is the factorial function, and ω_0, ω_1, ω_2 are the weighted moments of D_i, which are calculated as follows:

$$\omega_s = \frac{1}{N}\sum_{i=1}^{N}(1-F_i)^s D_i \tag{9}$$

$$F_i = \frac{i-0.35}{N} \tag{10}$$

where N is the number of months in the study.

Finally, the cumulative probability density is standardized:

$$\mathrm{P} = 1 - F_x \tag{11}$$

When the probability density $P \leq 0.5$:

$$\omega = \sqrt{-2\ln P} \tag{12}$$

$$\mathrm{SPEI} = \omega - \frac{c_0 - c_1\omega - c_2\omega^2}{1 + d_1\omega + d_2\omega^2 + d_3\omega^3} \tag{13}$$

where $c_0 = 2.515517$, $c_1 = 0.802853$, $c_2 = 0.010\ 328$, $d_1 = 1.432788$, $d_2 = 0.189269$, and $d_3 = 0.001308$.

If $P > 0.5$, the value of P can be represented by 1 – P:

$$\mathrm{SPEI} = -\left(\omega - \frac{c_0 - c_1\omega - c_2\omega^2}{1 + d_1\omega + d_2\omega^2 + d_3\omega^3}\right) \tag{14}$$

Drought frequency

The formula for calculating the drought frequency P is as follows:

$$\mathrm{P}_i = (n/m) * 100\% \tag{15}$$

where n is the number of droughts in the data series, and m is the number of data series.

Drought classification

Table 1 shows the drought classification of the SPEI values (McKee *et al.* 1993).

Trend analysis

The linear trend analysis in this study utilized two methods: linear trend estimation and the Mann–Kendall trend test. Linear trend estimation was used to analyze the inter-annual change trends of SPEI values at different time scales in Shandong Province. The Mann–Kendall test is a non-parametric test method recommended by the World Meteorological Organization for type variables and order variables (Yue *et al.* 2002). Here, the Mann–Kendall method was employed to test the significance of the change trends. When the Mann–Kendall method statistic Z is >0, it indicates an upward trend; when it is <0, it is a downward trend. When the absolute value of Z is ≥1.64 or ≥2.32, this indicates that the 95 and 99% reliability tests are exceeded, respectively.

The linear tendency estimation formula is as follows:

$$Y(t) = \mathrm{at} + \mathrm{b}, \tag{16}$$

where Y is the SPEI value, t is the time, a is the linear trend term, and a × 10 is the change of the SPEI value every 10a,

Table 1 | Classification of SPEI drought categories

Drought category	Extreme drought	Severe drought	Moderate drought	Slight drought
SPEI value	≤ −2.0	−2.0 to −1.5	−1.5 to −1.0	−1.0 to −0.5

which is the inter-annual tendency rate. When $a > 0$, this indicates that the SPEI numerical sequence increases with time, and when $a < 0$, this indicates that the SPEI numerical sequence decreases with time. The larger the absolute value, the more obvious the change trend. a is calculated based on the principle of the least-squares method.

Periodic wavelet analysis

Wavelet analysis is a method that incorporates time–frequency and multi-level resolution functions, which can effectively capture the periodic characteristics of different time scales of hydrometeorological series (Zhang *et al.*, 2008), reflect the periodic changes of meteorological elements, and predict the future development trend of hydrometeorological series. In this study, the Morlet wavelet was used to analyze the periodic changes of drought in Shandong Province at different time scales, while the cross-wavelet transform (XWT) and wavelet transform coherence spectrum were utilized to explore the multi-time scale correlation between the SPEI and atmospheric circulation indices. The mother wavelet used in the wavelet analysis was the standard Morlet wavelet; the specific methods and processes are detailed in the literature (Torrence & Compo 1998).

RESULTS

Analysis of the temporal characteristics of drought in Shandong Province

Analysis of the temporal evolution of drought at multiple time scales in Shandong Province

The SPEI features multiple time scale characteristics. Shandong Province is located in the temperate monsoon climate zone, experiencing long winters and summers. The seasonal and inter-annual distributions of precipitation are very uneven. Therefore, the monthly scale, seasonal scale, and annual scale SPEI (SPEI-1, SPEI-3, and SPEI-12, respectively) were selected to study the temporal variations of drought in this region (Figure 4). There were obvious differences in the sensitivity of the SPEI with time at different time scales in Shandong Province. The smaller the time scale, the more significant the change, and the greater the fluctuation range. SPEI-1 exhibited the largest fluctuations during the 1961–2017 study period, and the fluctuation period of SPEI-3 was longer than that of SPEI-1, reflecting the seasonal change law of Shandong's dry and wet periods. The change trend of SPEI-12 was relatively stable.

SPEI-1 changes are related to monthly temperature and moisture changes and reflect the soil water content during this period, thus providing a basis for formulating agricultural irrigation cycles (Ma *et al.* 2020). From 1961 to 2017, the overall SPEI-1 value of Shandong Province exhibited a significant decreasing trend, at a rate of −0.0637/ decade ($p < 0.01$). After 1995, the drought intensity increased more obviously, and the extreme drought events (SPEI < -2) all appeared after 2000 (Figure 4(a)).

SPEI-3 is mainly affected by seasonal precipitation and temperature changes, revealing the water content of the lower soil layer (Gao *et al.* 2017). The SPEI-3 values of spring, summer, autumn, and winter all displayed downward trends, at rates of −0.0786/ decade, −0.0823/ decade, −0.1427/ decade ($p < 0.05$), and −0.038/ decade. Of these, the SPEI decreasing trend was the most obvious in autumn, while the decreasing trend of the winter SPEI value was the slowest (Figure 4(b)–4(e)). According to the Mann–Kendall mutation test of the autumn SPEI (Figure 5(a)), it is obvious that most forward (UF) values were below 0, with a trend of decrease increase-decrease and a general trend of slow decrease within fluctuations. Two mutation points occurred in 1964 and 1977. The former signaled increasing SPEI values, while the latter indicated that after 1977, the autumn SPEI value began to mutate and decrease.

The changes of SPEI-12 reflect the inter-annual change characteristics of drought in Shandong Province, which better explain the change of river runoff and soil moisture in the lower layer (Zhao *et al.* 2015). From 1961 to 2017, the value of SPEI-12 in Shanding Province fluctuates frequently, and had maximum range fluctuations. The overall trend was downward, at a rate of −0.15333/decade ($p < 0.05$) (Figure 4(f)). The SPEI-12 displayed obvious phase characteristics. In 1965, 1970, and 1980, the SPEI-12 showed clear turning point, displaying a trend of up-down-up-down. From 1961 to 2017, the main drought periods in

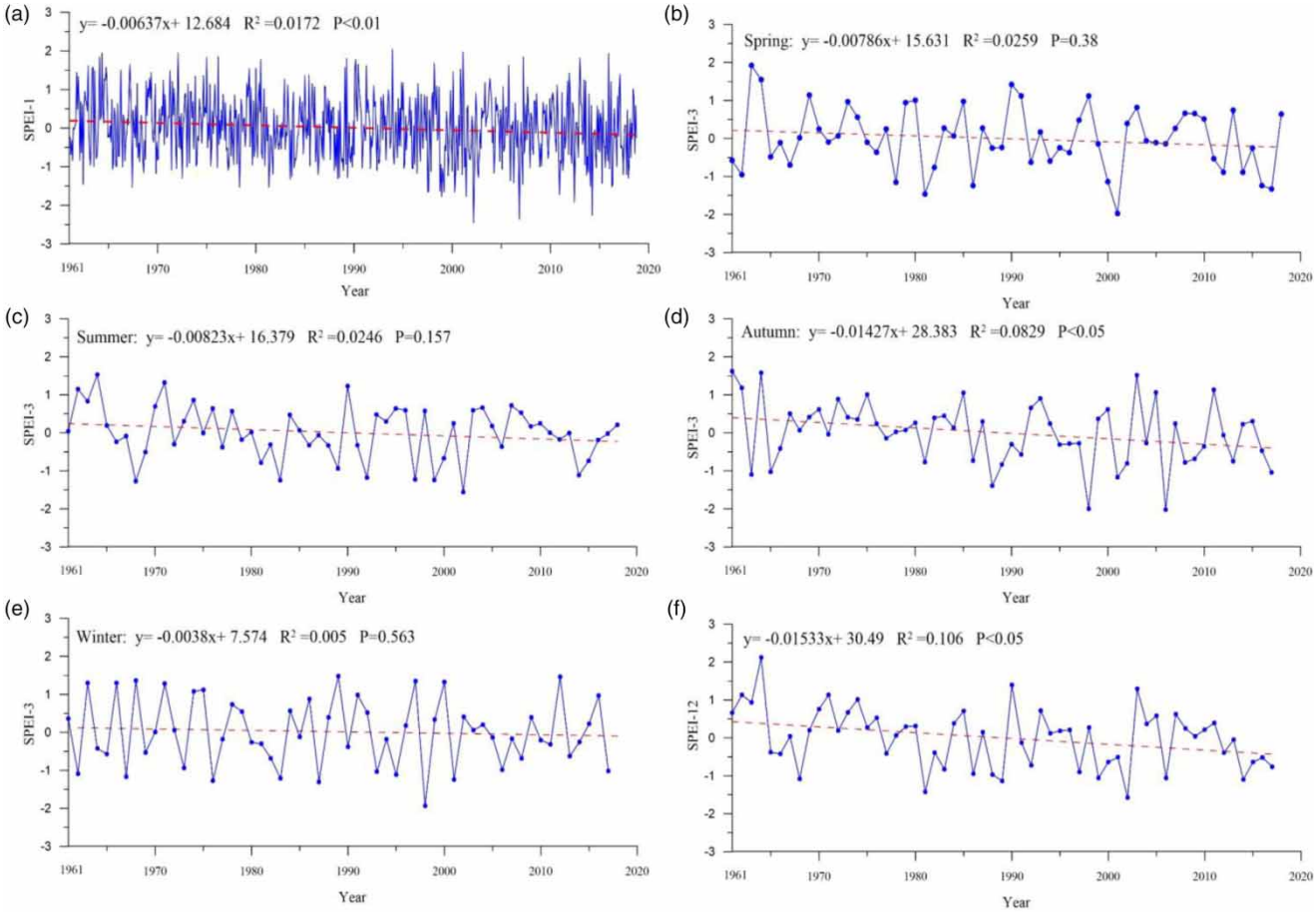

Figure 4 | SPEI values at different time scales in Shandong Province from 1961 to 2017: (a) SPEI-1, (b) SPEI-Spring, (c) SPEI-Summer, (d) SPEI-Autumn, (e) SPEI-Winter, (f) SPEI-12.

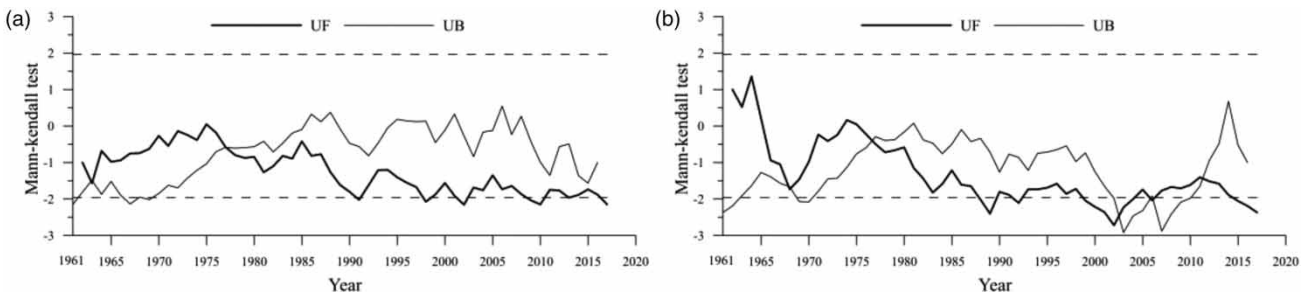

Figure 5 | Mann–Kendall test for SPEI-Autumn (a) and SPEI-12 (b) series in Shandong Province from 1961 to 2017. Horizontal dashed lines are the confidence limits (0.05).

Shandong Province were concentrated between 1980–1993, 1997–2004, and 2013–2017, among which 1968, 1981, 1989, 1999, and 2014 had higher drought intensities. The SPEI-12 values for these years reached −1.08, −1.43, −1.14, −1.06, and −1.10 manifesting as moderate drought, which were more consistent with the historical drought years in Shandong Province. The Mann–Kendall mutation test was performed on the SPEI-12 values in Shandong Province (Figure 5(b)). The mutation points appeared in 1968, 1977, and 2013. The mutation points in 1977 and 2013 all indicated that the drought exhibited increasing trends following these years.

Analysis of drought periodicity in Shandong Province

In order to study the characteristics of drought periodicity at multiple time scales in Shandong Province, the SPEI-3 and SPEI-12 were examined using Morlet wavelet analysis. Figures 6 and 7 illustrate the contour plots of the real part of the wavelet coefficients and wavelet variance, respectively.

It can be seen from Figure 6 that the SPEI (annual and four seasons) of Shandong Province from 1961 to 2017 contained periodic changes, with obvious alternations of dry and wet. There were small-scale signals with periods of 3–6 years and large-scale signals with periods of 8–12 years and 25–32 years in SPEI during the spring (Figure 6(a)). The positive and negative phase periods of the three wavelet period scales were readily apparent during the spring, all of which were global and stable. There were three peaks in the spring wavelet variance map, corresponding to time scales of 4, 8, and 29 years, only the 8 years scale passes the 0.05 confidence level test (Figure 7(a)), so the 8 years scale was the first major cycle of spring drought change in Shandong Province.

In summer, there were small-scale signals with 3–5 years and 5–8 years periods in SPEI, large-scale signals

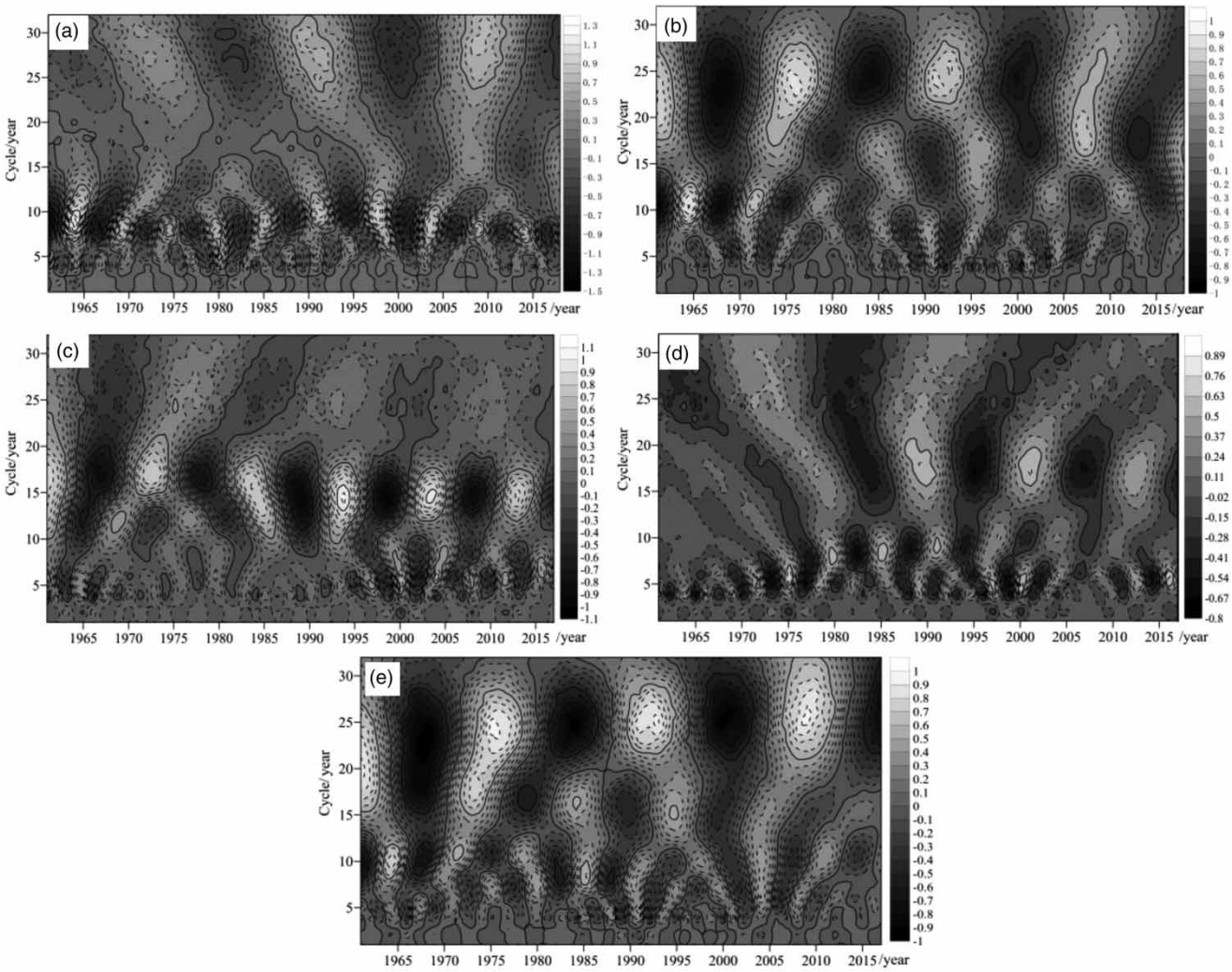

Figure 6 | Morlet wavelet analysis for SPEIs at different time scales in Shandong Province from 1961 to 2017: (a) SPEI-Spring, (b) SPEI-Summer, (c) SPEI-Autumn, (d) SPEI-Winter, (e) SPEI-12.

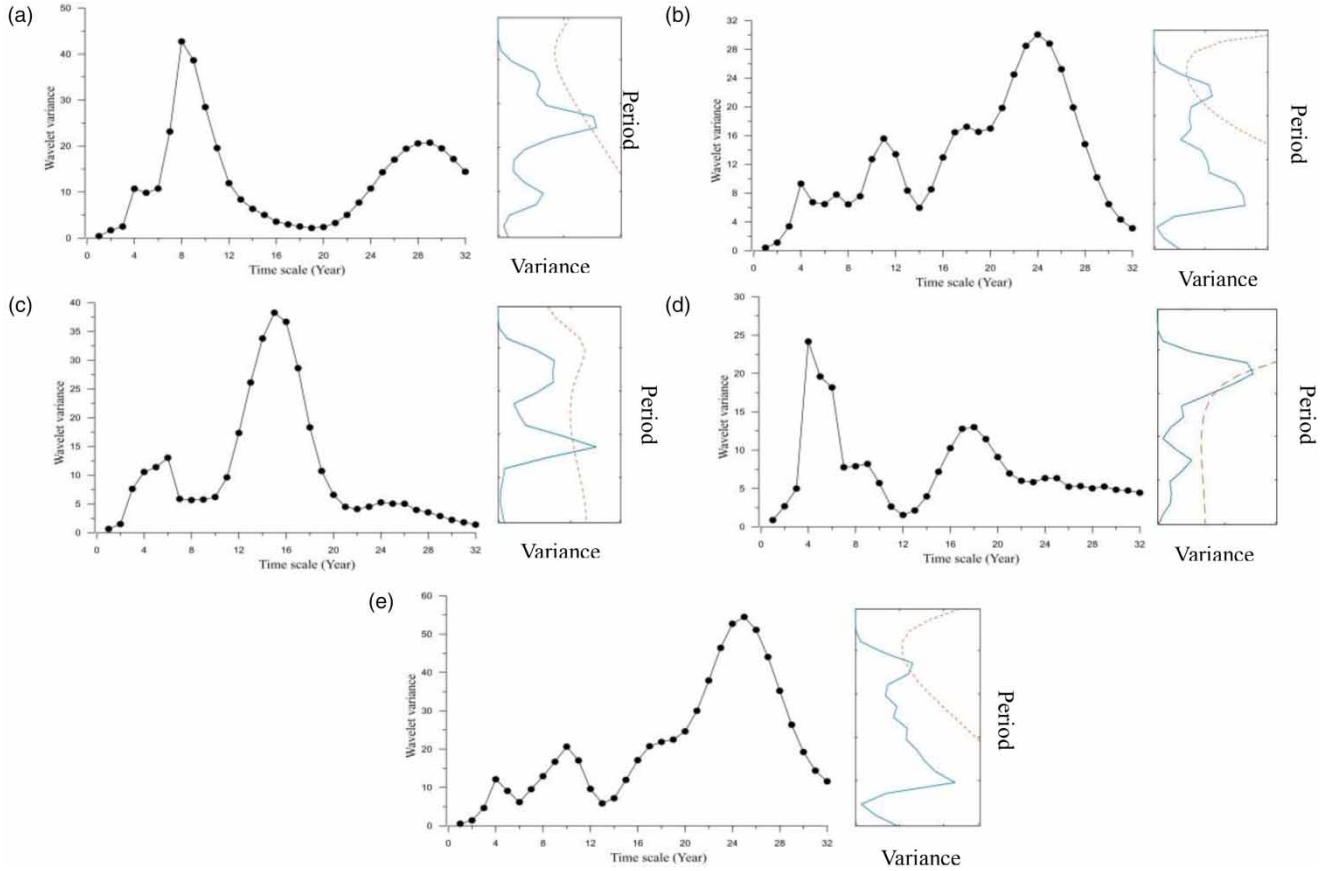

Figure 7 | Wavelet variance for SPEIs in Shandong Province from 1961 to 2017: (a) SPEI-Spring, (b) SPEI-Summer, (c) SPEI-Autumn, (d) SPEI-Winter, (e) SPEI-12. (The dotted line on the right designated the significance level $\alpha = 95\%$ against red noised.)

with 8–15 years and 17–30 years periods, and obvious alternations of dry and wet at four scales (Figure 6(b)). There were four peaks in the summer wavelet variance map, corresponding to the time scales of 4, 11, 18, and 24 years, and only the 4 years scale passes the 0.05 confidence level test (Figure 7(b)), so the 4 years scale was the first major cycle of summer drought change in Shandong Province.

In autumn, there were small-scale signals with 3–8 years periods in SPEI, large-scale signals with 10–20 years periods, and a total of 12.5 alternating dry and wet changes (Figure 6(c)). There were two peaks in the autumn wavelet variance map, corresponding to the time scales of 6 years and 15 years, and only the 15 years scale passes the 0.05 confidence level test (Figure 7(c)), so the 15 years scale was the first major cycle of autumn drought change in Shandong Province.

In winter, the SPEI exhibited small-scale signals of 3–5 years and 6–10 years, and large-scale signals of 14–32 years, and a total of 8.5 dry and wet alternations (Figure 6(d)). There were three peaks in the winter wavelet variance map, corresponding to the time scales of 4 years, and only the 4 years scale passes the 0.05 confidence level test (Figure 7(d)), so the 4 years scale was the first major cycle of winter drought change in Shandong Province.

SPEI-12 displayed small-scale signals of 3–6 years and large-scale signals of 7–13 years and 15–33 years, and there were 7.5 alternating dry and wet changes (Figure 6(e)). There were three peaks in the SPEI-12 wavelet variance map, corresponding to time scales of 4 years, 10 years, and 25 years, and only the 4 years scale passes the 0.05 confidence level test (Figure 7(d)), so the 4 years scale was the first major cycle of inter-annual drought change in Shandong Province.

Analysis of the spatial characteristics of drought in Shandong Province

Analysis of the spatial characteristics of drought at different time scales in Shandong Province

Based on the calculation results of multi-time scale SPEIs in Shandong Province, combined with ArcGIS software, the spatial distribution characteristics of drought frequency at different scales in the region were analyzed. Overall, the frequency of monthly drought ranged from 32% to 36.5%, and the frequency of drought manifested an increasing trend from northwest to southeast (Figure 8(a)). On the seasonal scale, spring drought mainly occurred in the northern, central, and southwestern regions of Shandong Province, and the frequency of drought on the southwest region of Shandong Province was the lowest, 25.86% (Figure 8(b)). The drought frequency in summer (25.5%–36.5%) was slightly higher than that in spring, with droughts mainly occurring in northern and southeastern Shandong Province, and the lowest value 25.5% occurring on the southwest and central regions (Figure 8(c)). The frequency of drought was highest in the autumn, ranged from 28% to 40.5%, and the high-frequency areas were mainly concentrated in eastern Shandong (Figure 8(d)). The frequency of drought in winter was slightly lower than that in autumn and was mainly concentrated in eastern Shandong, which reached 40.35%, while other regions consistently ranged from 25% to 33% (Figure 8(e)). At the annual scale, regional differences were relatively large at drought occurrence frequency and unevenly distributed in Shandong Province, and the frequency of drought occurrence was relatively high in the central, south and northwest of Shandong Province, all more than 35%, and the lowest value 26% occurring on the southwest of Shandong Province (Figure 8(f)).

Spatial distribution characteristics of different drought types at different time scales

Figure 9(a1)–9(a4) present the distributions of different drought types in Shandong Province on the monthly scale from 1961 to 2017. The frequency of slight drought ranged from 14% to 20%, and moderate and above-moderate droughts exhibiting an increasing trend from northwest to southeast. The frequency of slight drought in spring ranged from 5% to 20%, exhibiting a high-low-high distribution pattern from west to east, the frequency of moderate and severe

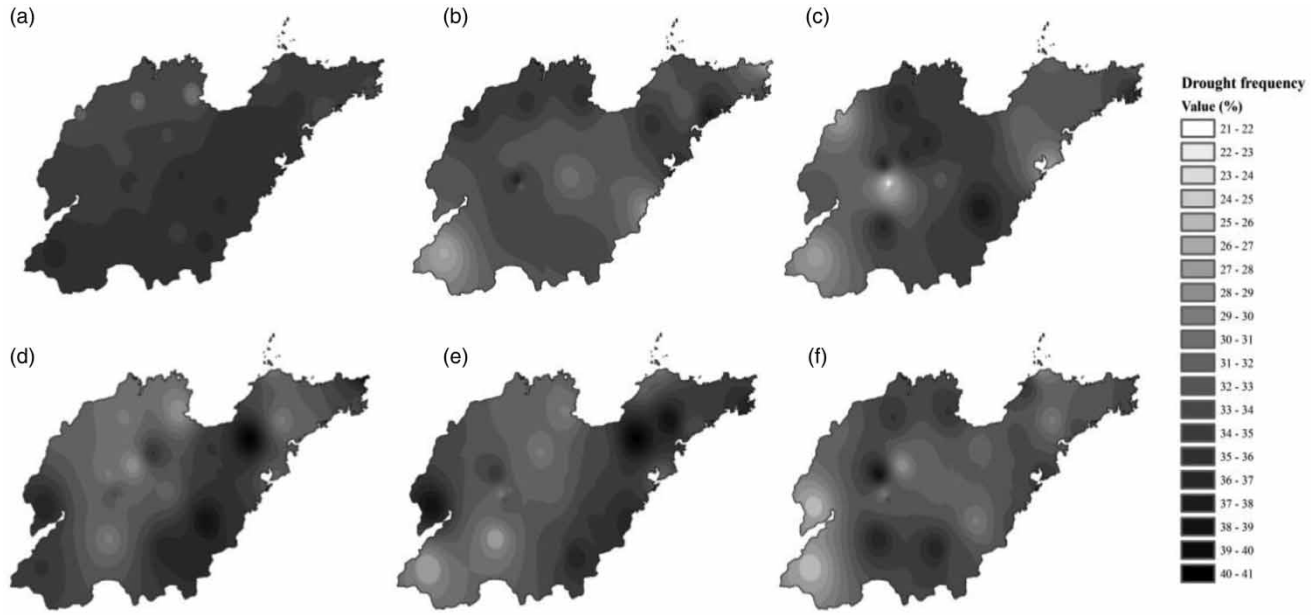

Figure 8 | Drought frequency distributions at different time scales in Shandong from 1961 to 2017: (a) Monthly, (b) Spring, (c) Summer, (d) Autumn, (e) Winter, and (f) Annual.

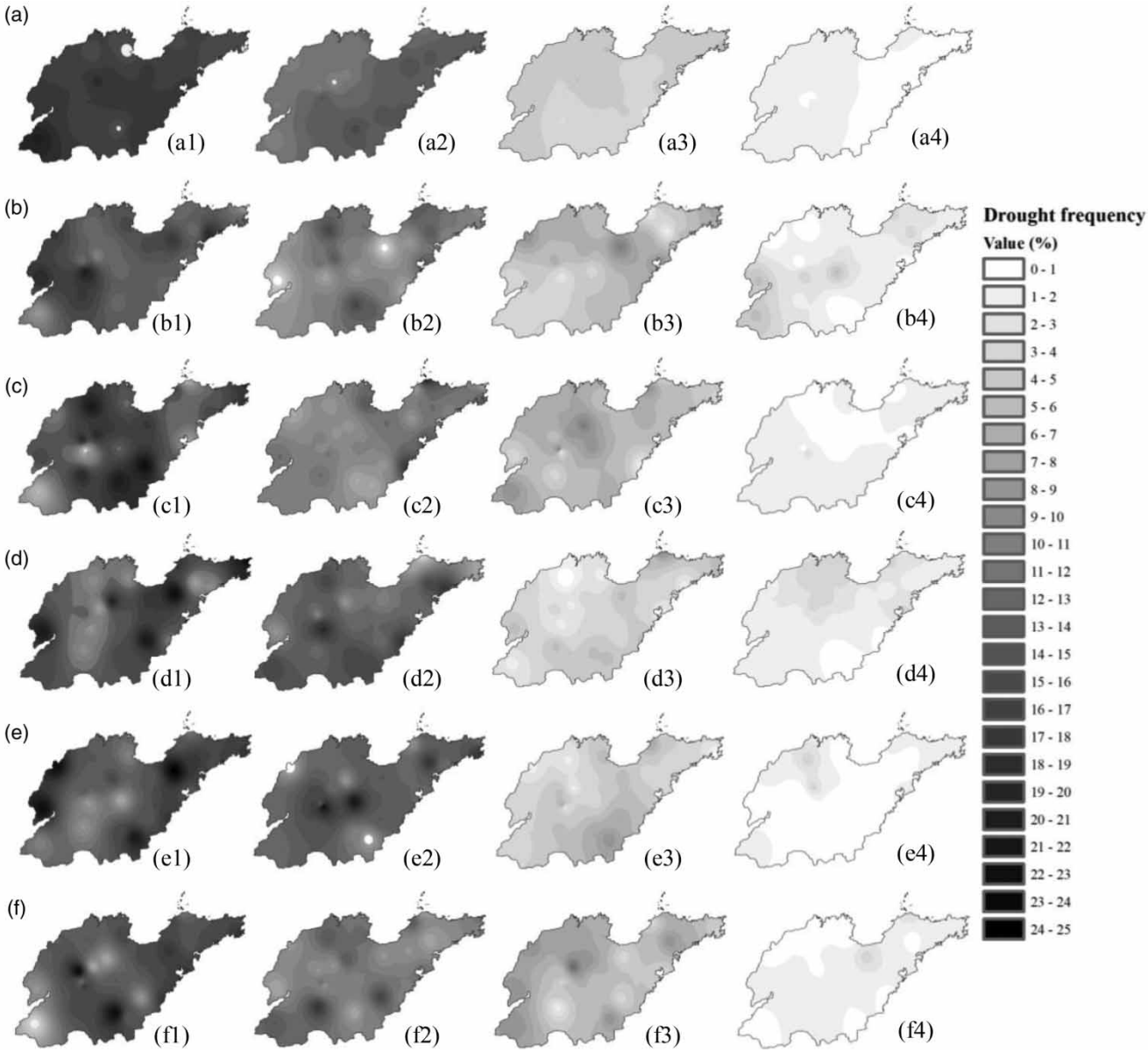

Figure 9 | Drought frequency distributions of different scales and grades in Shandong Province from 1961 to 2017: (a) Monthly, (b) Spring, (c) Summer, (d) Autumn, (e) Winter, and (f) Annual, (1) Slight drought, (2) Moderate drought, (3) Severe drought, and (4) Extreme drought.

drought on the southwest region was the lowest, approximately 1–5% (Figure 9(b1)–9(b4)). In summer, the high-frequency area of slight drought was mainly concentrated in the central part of the province, while moderate drought was the opposite, and there was almost no extreme drought in the northern part of Shandong Province (Figure 9(c1)–9(c4)). In autumn, the frequency of slight drought ranged from 8% to 23%, which was the highest of the four seasons, the frequency of moderate and severe drought on the southwest and south region was the highest, 19% and 10.5% respectively (Figure 9(d1)–9(d4)). In winter, the frequency of slight drought ranged from 6% to 23%, which exhibited a high-low-high distribution pattern from northwest to southeast, the frequency of moderate drought varied between 7 and 23%, which was the highest of the four seasons (Figure 9(e1)–9(e4)). At the annual scale, the

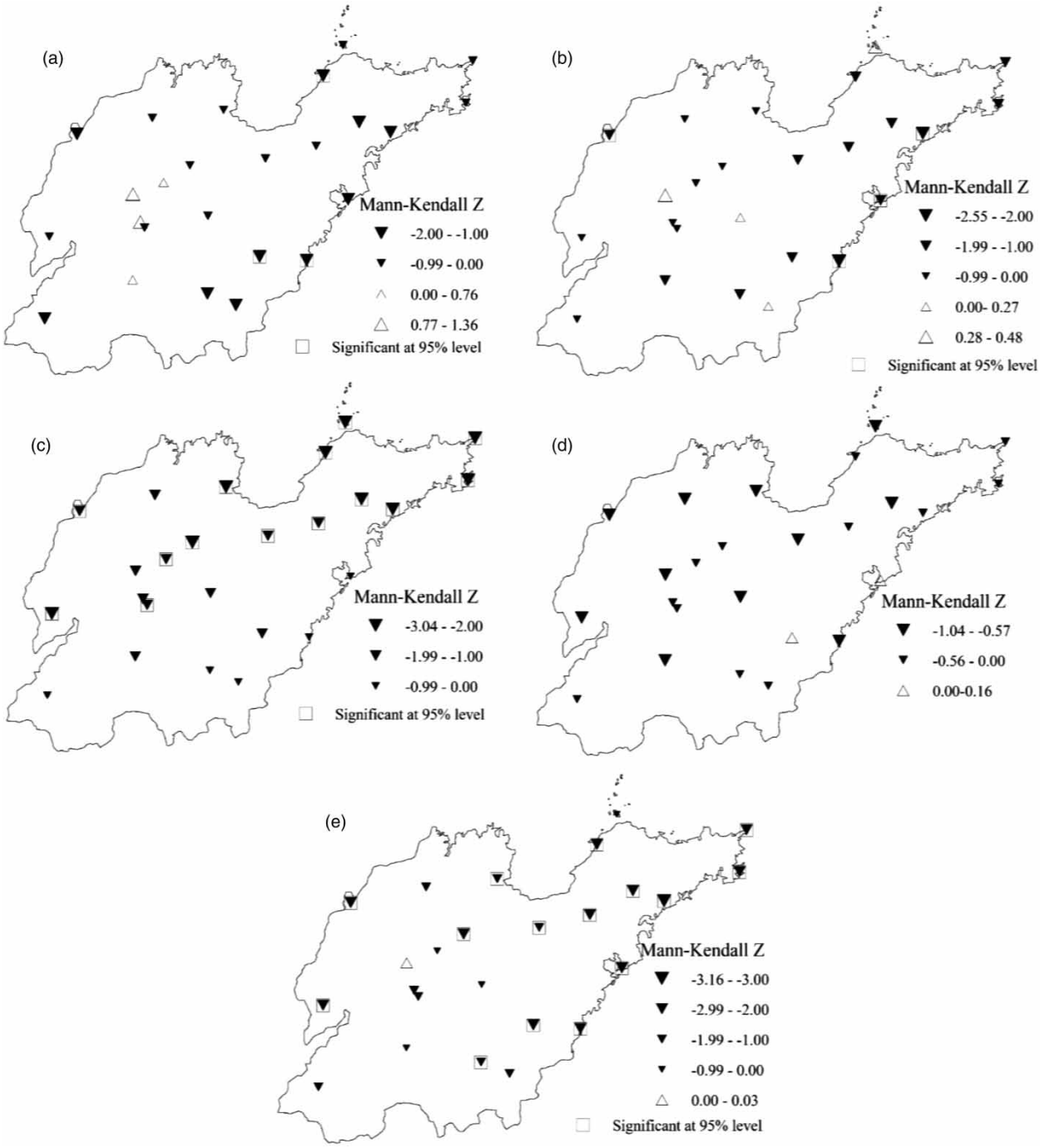

Figure 10 | Drought index change trends at different scales in Shandong Province from 1961 to 2017: (a) Spring, (b) Summer, (c) Autumn, (d) Winter, (e) Annual.

frequency of slight drought in southwestern Shandong Province experiencing generally low frequencies of ~5%, the frequency of moderate drought was relatively high in central region, and no extreme drought occurred in northern and southwestern Shandong Province (Figure 9(f1)–9(f4)).

Analysis of the spatial trends of drought in Shandong Province

In order to further analyze the spatial distribution characteristics of drought change trends in Shandong Province, the Mann–Kendall statistical Z-values of the 57-year seasonal scale and annual scale SPEI values of each meteorological station were calculated, and an SPEI Z-value spatial distribution map was then generated using ArcGIS software (Figure 10).

In spring, the SPEI values in the central and western regions of Shandong Province showed an upward trend, with a trend rate of (0.016–0.132)/decade, and the trend was not significant ($|Z| > 1.96$); the SPEI values in other regions showed a downward trend, with a trend rate of (−0.155 to −0.012)/decade, and only 14.3% of the stations passed the 0.05 significance level test, mainly distributed in the southeast and northeast coastal area. In summer, the trend rate of SPEI values were between (−0.208–0.046)/decade, and 84 and 16% of the stations with downward trend and upward trend respectively. Among them, four stations show a significant downward trend ($|Z| > 1.96$), mainly distributed in the southeast coastal area. In autumn, the SPEI values in all regions of Shandong Province showed a downward trend, with a trend rate of (−0.245 to −0.058)/decade, and 56% of the stations show a significant downward trend ($|Z| > 1.96$), mainly distributed in the in the central and eastern regions. In winter, the trend rate of SPEI values were between (−0.08–0.013)/decade, and the downward and upward trends account for 92 and 8% respectively, with none of the stations failing the 0.05 significance level test. On the annual scale, only one stations in central Shandong showed an upward trend, and the trend rate was 0.0037/decade, and the trend was not significant; the SPEI values in other regions showed a downward trend, with a trend rate of (−0.256 to −0.041)/decade, and 15 stations passed the 0.05 significance level test, mainly distributed in eastern and southeastern regions of Shandong Province.

Teleconnection relationship between SPEI value and large-scale atmospheric circulation

This study used the Pearson correlation method to compare the monthly SPEI with the Southern Oscillation (SOI), North Atlantic Oscillation (NAO), Arctic Oscillation (AO), Pacific Decadal Oscillation (PDO), Sunspot number (SN), MEI and EASM (Figure 11), facilitating exploration of the causes of meteorological drought in Shandong Province. It can be seen from Figure 11 that Shandong Province was affected by different atmospheric circulation indices in different months during the study period, and there were multiple atmospheric circulation indices in some months that exerted a compound effect. Among them, the correlation coefficients between the SN and MEI and the monthly SPEI values were generally large. In order to further understand the impact of SN and MEI on SPEI, cross-wavelet transform and coherent-wavelet transform were performed on the time series of SPEI, MEI, and SN at the monthly scale for Shandong Province, and their relationship was analyzed in terms of time-frequency.

Figures 12 and 13 show the cross-wavelet change (Figures 12(a) and 13(a)) and coherent-wavelet change (Figures 12(b) and 13(b)) of the monthly scale SPEI and MEI and SN. Figure 12(a) indicates that there were resonance periods of 2–3.5 years and 1.8–4 years between the SPEI and MEI from 1966 to 1972 and 1987 to 1992. The phase angle reveals that the SPEI and MEI had a positive phase in the first period. The SPEI lagged the MEI by 6 months in the second period. Figure 12(b) shows that there was a resonance period of 3.3–4 years between the

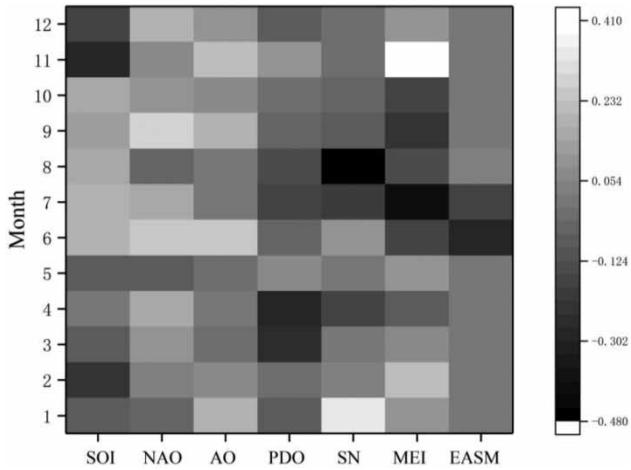

Figure 11 | Pearson correlation coefficients between monthly-scale SPEI values and atmospheric circulation indices in Shandong Province from 1961 to 2017.

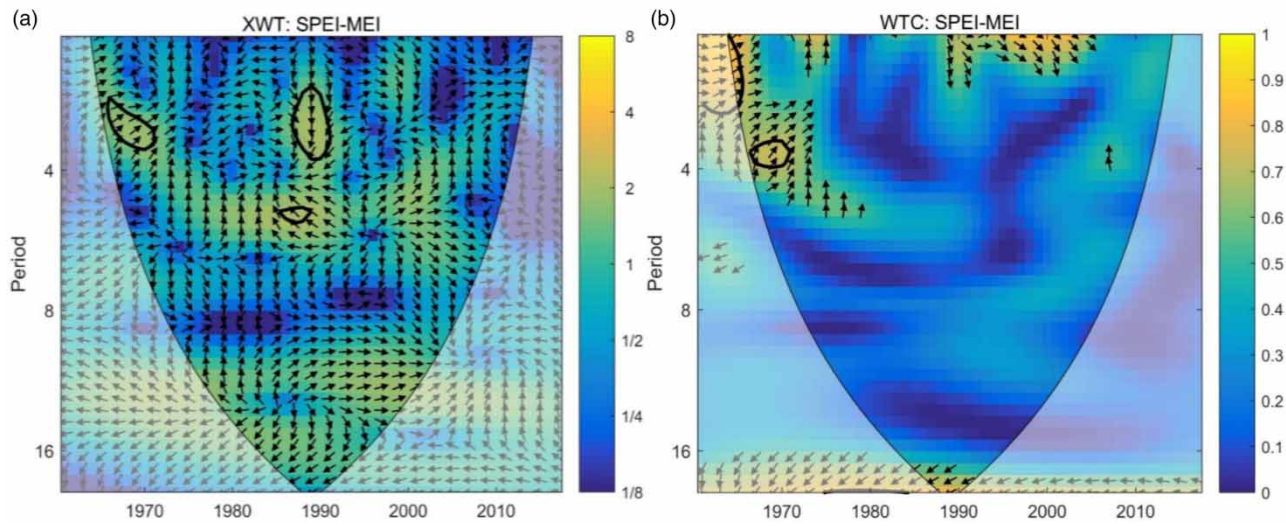

Figure 12 | Cross-wavelet transforms (a) and coherent-wavelet transforms (b) of the SPEI and MEI (The thick black contours depict the 5% confidence level, and the black line is the cone of influence. Right-pointing arrows indicate that the two signals are in phase, while left-pointing arrows indicate anti-phase signals. Down-pointing arrows indicate that the MEI is ahead of the SPEI, while up-pointing arrows indicate that the MEI lags behind the SPEI.).

SPEI and MEI in the low-energy region of the coherent wavelet from 1968 to 1971. Figure 13(a) indicates that there was a resonance period of 8.5–13 years between the SPEI and SN in the high energy region of the cross-wavelet from 1974 to 2003, The phase angle reveals that the SPEI ahead the MEI by 6 months. Figure 13(b) shows that there were resonance periods of 3.8–5 years and 11–13 years between the SPEI and SN from 1978 to 1982 and 1985 to 1998 in the low-energy region of the coherent wavelet. The phase angle reveals that the SPEI and SN displayed a positive phase during the first cycle while leading by 6 months in the second cycle.

CONCLUSIONS

Based on the data from 25 meteorological stations in Shandong Province for the period 1961–2017, using the methods

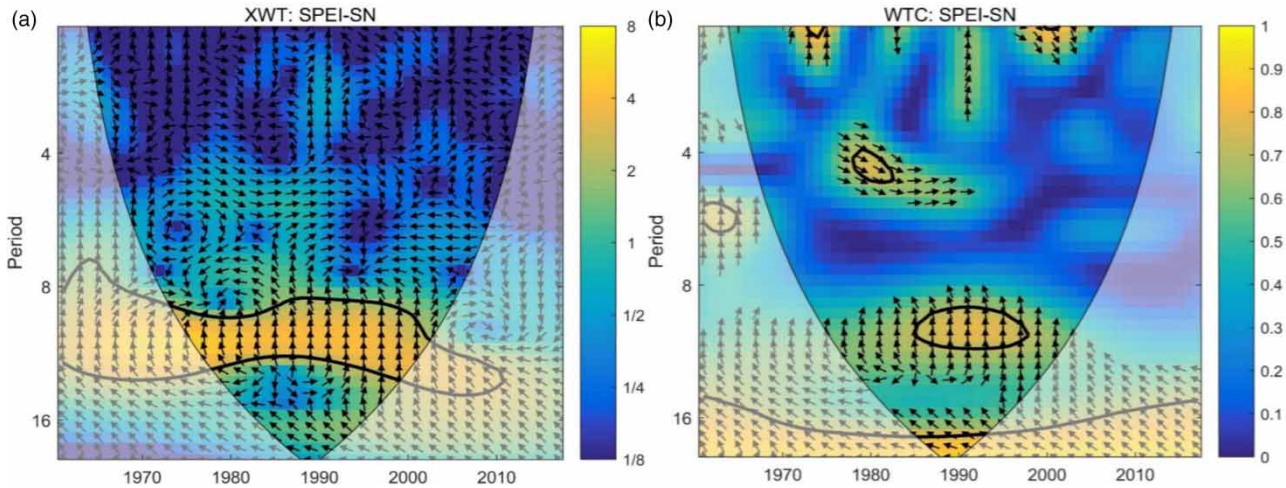

Figure 13 | Cross-wavelet transforms (a) and coherent-wavelet transforms (b) of the SPEI and SN. (The thick black contours depict the 5% confidence level, and the black line is the cone of influence. Right-pointing arrows indicate that the two signals are in phase, while left-pointing arrows indicate anti-phase signals. Down-pointing arrows indicate that the SN is ahead of the SPEI, while up-pointing arrows indicate that the SN index lags behind the SPEI.)

of trend analysis, correlation analysis, and wavelet analysis, the spatial and temporal changes and periodic changes of drought in Shandong Province were analyzed at the annual, seasonal, and monthly scales, and the influences of atmospheric circulation indices on these drought changes were explored. The main conclusions are as follows.

(1) SPEI values can better reflect the spatiotemporal characteristics of drought changes and identify and characterize historical drought events in Shandong Province. In terms of time scale, the monthly, seasonal, and annual scales of the SPEI values exhibited decreasing trends, and the drought years represented by the SPEI-12 value was consistent with the historical drought years in Shandong Province. The spatial distribution of drought frequency at different scales was significantly different. The frequency of drought occurrence at the annual scale was relatively high in the central, south and northwest of Shandong Province.
(2) From 1961 to 2017, the decrease of precipitation and the increase of temperature and the SPEI values of all scales showed a downward trend in Shandong Province, which showed the possibility of further aggravation of drought in Shandong Province in the future. This is likely to have detrimental impacts on the water supply, agriculture and social economy of Shandong Province. The results of this paper can provide reference for local government departments to prevent drought and manage water resources.

ACKNOWLEDGEMENTS

This work was supported by the National Natural Science Foundation of China (No. 41471160) and the Natural Science Foundation of Shandong Province (ZR2019BEE064). The authors would also like to thank the reviewers for their very valuable comments, which greatly improved the quality of this manuscript.

DECLARATION OF COMPETING INTEREST

The authors declare no conflicts of interest.

DATA AVAILABILITY STATEMENT

Data cannot be made publicly available; readers should contact the corresponding author for details.

REFERENCES

Aghakouchak, A., Cheng, L. Y., Mazdiyasni, O. & Farahmand, A. 2014 Global warming and changes in risk of concurrent climate extremes: insights from the 2014 California drought. *Geophysical Research Letters* **41** (24), 8847–8852. https://doi.org/10.1002/2014GL062308.

Bongaarts, J. 2018 Special report on climate change and land use. intergovernmental panel on climate change, 2018. *Population and Development Review* **45** (4), 936–937. https://doi.org/10.1111/padr.12306.

Chen, H. P., Sun, J. Q. & Chen, X. L. 2013 Future changes of drought and flood events in China under a global warming scenario. *Atmospheric & Oceanic Science Letters* **6** (1), 8–13. (In Chinese).

Cook, B. I., Smerdon, J. E., Seager, R. & Coats, S. 2014 Global warming and 21st century drying. *Climate Dynamics* **43** (9–10), 2607–2627. https://doi.org/10.1007/s00382-014-2075-y.

Gao, X. R., Zhao, Q., Zhao, X. N., Wu, P., Pan, W. X., Gao, W. X. & Sun, M. 2017 Temporal and spatial evolution of the standardized precipitation evapotranspiration index (SPEI) in the Loess Plateau under climate change from 2001 to 2050. *Science of the Total Environment* **595**, 191–200. https://doi.org/10.1016/j.scitotenv.2017.03.226.

Guo, H., Bao, A., Liu, T., Jiapaer, G. L., Ndayisaba, F., Jiang, L. L., Kurban, A. & Maeyer, P. 2018 Spatial and temporal characteristics of droughts in Central Asia during 1966–2015. *Science of the Total Environment* **624**, 1523–1538. https://doi.org/10.1016/j.scitotenv.2017.12.120.

Hao, Z. C., AghaKouchak, A., Nakhjiri, N. & Farahmand, A. 2014 Global integrated drought monitoring and prediction system. *Scientific Data* **1**, 140001. https://doi.org/10.1038/sdata.2014.1.

Hayes, M., Svoboda, M., Wall, N. & Widhalm, M. 2011 The Lincoln declaration on drought indices: universal meteorological drought index recommended. *Bulletin of the American Meteorological Society* **92** (4), 485–488. https://doi.org/10.1175/2010bams3103.1.

Jiang, P. Y., Chen, X. L., Li, Q. Y., Mo, H. H. & Li, L. Y. 2020 High-resolution emission inventory of gaseous and particulate pollutants in Shandong Province, Eastern China. *Journal of Cleaner Production* **259**, 120806. https://doi.org/10.1016/j.jclepro.2020.120806.

Li, Q. X., Dong, W. J. & Jones, P. 2020 Continental scale surface air temperature variations: experience derived from the Chinese region. *Earth-Science Reviews* **200**, 102998. https://doi.org/10.1016/j.earscirev.2019.102998.

Ma, B., Zhang, B., Jia, L. J. & Huang, H. 2020 Conditional distribution selection for SPEI-daily and its revealed meteorological drought characteristics in China from 1961 to 2017. *Atmospheric Research* **246**, 105108. https://doi.org/10.1016/j.atmosres.2020.105108.

McKee, T. B., Doesken, N. J. & Kleist, J. 1993 The relationship of drought frequency and duration to time scales. *Eighth Conference on Applied Climatology* **1**, 17–22.

Palmer, W. C. 1965 *Meteorological Drought*. Research Paper 45, U.S. Department of Commerce, Weather Bureau, Washington, DC, p. 58.

Schär, C., Ban, N., Fischer, E. M., Rajczak, J., Schmidli, J., Frei, C., Giorgi, F., Sillmann, J., Zhang, X. B., Fischer, E. M., Karl, T. R., Kendon, E. J., Tank, A. M. G. K., Zwiers, F. W. & O'Gorman, P. 2016 Percentile indices for assessing changes in heavy precipitation events. *Climatic Change* **137** (1/2), 201–216. https://doi.org/10.1007/s10584-016-1669-2.

Shi, J., Cui, L. L. & Tian, Z. 2020 Spatial and temporal distribution and trend in flood and drought disasters in East China. *Environmental Research* **185**, 109406. https://doi.org/10.1016/j.envres.2020.109406.

Tan, C. P., Yang, J. P. & Li, M. 2015 Temporal-spatial variation of drought indicated by SPI and SPEI in Ningxia Hui Autonomous Region, China. *Atmosphere (Basel)* **6** (10), 1399–1421. https://doi/10.3390/atmos6101399.

Torrence, C. & Compo, G. P. 1998 A practical guide to wavelet analysis. *Bulletin of American Meteorological Society* **79** (1), 61–78. https://doi.org/10.1175/1520-0477(1998)079 < 0061: APGTWA > 2.0.CO;2.

Vicente-Serrano, S. M. & López-Moreno, J. 2006 The influence of atmospheric circulation at different spatial scales on winter drought variability through a semi-arid climatic gradient in Northeast Spain. *International Journal of Climatology* **26** (11), 1427–1453. https://doi.org/10.1002/joc.1387.

Vicente-Serrano, S. M., Beguería, S. & López-Moreno, J. I. 2010 A multi-scalar drought index sensitive to global warming, The standardized precipitation evapotranspiration index-SPEI. *Journal of Climate* **23** (7), 1696–1718. https://doi.org/10.1175/2009JCLI.2009.1.

Wambua, R. M., Benedict, M. M. & James, R. M. 2017 Analysis of spatial and temporal drought variability in a tropical river basin using Palmer Drought Severity Index (PDSI). *International Journal of Water Resources and Environmental Engineering* **9** (8), 178–190. https://doi.org/10.5897/IJWREE2017.0723.

You, Q. L., Kang, S. C., Aguilar, E., Pepin, N., Flügel, W. A., Yan, Y. P., Wu, Y. W., Zhang, Y. J. & Huang, J. 2011 Changes in daily climate extremes in China and their connection to the large scale atmospheric circulation during 1961–2003. *Climate Dynamics* **36** (11–12), 2399–2417. https://doi.org/10.1007/s00382-009-0735-0.

Yu, M. X., Li, Q. F., Hayes, M. J., Svoboda, M. & Heim, R. 2014 Are droughts becoming more frequent or severe in China based on the standardized precipitation evapotranspiration index: 1951–2010? *International Journal of Climatology* **34** (3), 545–558. https://doi.org/10.1002/joc.3701.

Yue, S., Pilon, P. & Cavadias, G. 2002 Power of the Mann–Kendall and Spearman's rho tests for detecting monotonic trends in hydrological series. *Journal of Hydrology* **259** (1–4), 254–271. https://doi.org/10.1016/S0022-1694(01)00594-7.

Zhang, Y. M. & Diao, X. S. 2020 The changing role of agriculture with economic structural change – the case of China. *China Economic Review* **62**, 101504. https://doi.org/10.1016/j.chieco.2020.101504.

Zhang, J. H., Wei, F. Q., Liu, S. Z. & Gao, C. 2008 Possible effect of ENSO on annual sediment discharge of debris flows in the Jiangjia Ravine based on Morlet wavelet transforms. *International Journal of Sediment Research* **23** (3), 267–274. https://doi.org/10.1016/S1001-6279(08)60024-4.

Zhao, H. Y., Gao, G., An, W., Zou, X. K., Li, H. T. & Hou, M. T. 2015 Timescale differences between SC-PDSI and SPEI for drought monitoring in China. *Physics & Chemistry of the Earth Parts A/B/C* **102**, 48–58. https://doi.org/10.1016/j.pce.2015.10.022.

Zhao, Z. Y., Wang, H. R., Yu, C., Deng, C. N., Liu, C. L., Wu, Y. F., Yan, J. W. & Wang, C. 2020 Changes in spatiotemporal drought characteristics over northeast China from 1960 to 2018 based on the modified nested Copula model. *Science of The Total Environment* **739**, 140328. https://doi.org/10.1016/j.scitotenv.2020.140328.

First received 30 July 2020; accepted in revised form 8 November 2020. Available online 19 November 2020